Satellite-observed lake size trends around Asian Water Tower under a warming climate

Nuo Xu[1], Andre Daccache[2], Peng Gou[3], Chong Liu[4], Tianyu Zhou[3], Jiahua Zhang[5], Bo Zhou[1], Sierra Burkhurt[1], and Nie Wei[3]

[1]University of California Los Angeles
[2]University of California Davis
[3]Nanhu Laboratory
[4]Piesat Information Technology Co., Ltd.
[5]Institute of Remote Sensing and Digital Earth, Chinese Academy of Sciences, Beijing, China

November 24, 2022

Abstract

Recent studies suggest Asian Water Tower (AWT) is vulnerable to climate change with a detrimental effect on water and food security. Comprehensive information about the spatio-temporal variability of lakes, an important freshwater resource, is lacking. Therefore, we analyzed 89,480 Landsat images to examine the change in the lakes size around AWT between 1977±2 and 2020±2. Sequentially, the trends of precipitation, snow water equivalent, glacier mass, and permafrost were analyzed to understand what caused the lake's alteration. According to our findings, from 1977±2 to 2020±2, 84% of mapped lakes grew during the wet season, whereas 81% of the lakes grew during the dry season. Lakes in the Inner TP and Tarim Interior basins expanded dramatically. The Helmand, Amu Darya, and Yangtze basins are the primary locations of shrinking lakes. The Aral Sea shrunk by 90%. From the region as a whole, the alpine lakes showed a shrinking trend and the plain lakes showed an expanding trend from 1977±2 to 1990±2, and vice versa from 1990±2 to 2020±2. Glacial loss and permafrost thawing were corresponding to lake expansion in the Inner TP, Tarim Interior, Syr Darya, and Mekong basins. Permafrost discontinuities may cause Indus and Ganges to not grow significantly in lakes with increased recharge to the basin. Extreme droughts depleted the lake in Helmand. Human intervention have caused the shrinking of the Aral Sea and the lakes in the lower Yangtze River. As AWT retreats and feeds lakes, we need to take immediate action for managing risks and adaption.

Hosted file

`essoar.10512354.1.docx` available at https://authorea.com/users/551854/articles/604533-satellite-observed-lake-size-trends-around-asian-water-tower-under-a-warming-climate

Nuo Xu[1,2,3], Andre Daccache[4], Peng Gou[2,3], Chong Liu[5,6], Jiahua Zhang[7,8], Tianyu Zhou[2,3], Bo Zhou[1], Sierra Burkhart[1], Wei Nie[2,3]

[1]Department of Geography, University of California, Los Angeles, 90024, USA

[2]Big Data Technology Research Center, Nanhu Laboratory, Jiaxing, 314002, China

[3]Beijing Big Data Advanced Technology Institute, Beijing, 100871, China

[4]Department of Biological and Agricultural Engineering, University of California, Davis, 95616, USA

[5]Piesat Information Technology Co., Ltd., Beijing 100195, China

[6]Institute of Tibetan Plateau Research, Chinese Academy of Sciences, Beijing, 100101, China

[7]University of Chinese Academy of Sciences, Beijing, 100049, China

[8]Key Laboratory of Digital Earth Sciences, Aerospace Information Research Institute, Chinese Academy of Sciences, Beijing, 100101, China

Corresponding author: Andre Daccache (adaccache@ucdavis.edu); Peng Gou † (goupeng@nanhulab.ac.cn)

Key Points:

- 84% of the 209 large lakes around AWT expanded during the wet seasons from 1977±2 to 2020±2, while 81% grew during the dry seasons.
- Lakes in inner TP and Tarim basin grew dramatically. Helmand, Amu Darya and Yangtze basins are the main position of lake shrinkage.
- Changes in lake size are closely tied to trends in precipitation, snow water equivalent, glacier mass, permafrost.

Abstract

Recent studies suggest Asian Water Tower (AWT) is vulnerable to climate change with a detrimental effect on water and food security. Comprehensive information about the spatio-temporal variability of lakes, an important freshwater resource, is lacking. Therefore, we analyzed 89,480 Landsat images to examine the change in the lakes size around AWT between 1977±2 and 2020±2. Sequentially, the trends of precipitation, snow water equivalent, glacier mass, and permafrost were analyzed to understand what caused the lake's alteration. According to our findings, from 1977±2 to 2020±2, 84% of mapped lakes grew during the wet season, whereas 81% of the lakes grew during the dry season. Lakes in the Inner TP and Tarim Interior basins expanded dramatically. The Helmand, Amu Darya, and Yangtze basins are the primary locations of shrinking lakes. The Aral Sea shrunk by 90%. From the region as a whole, the alpine lakes showed a shrinking trend and the plain lakes showed an expanding trend from 1977±2 to 1990±2, and vice versa from 1990±2 to 2020±2. Glacial

loss and permafrost thawing were corresponding to lake expansion in the Inner TP, Tarim Interior, Syr Darya, and Mekong basins. Permafrost discontinuities may cause Indus and Ganges to not grow significantly in lakes with increased recharge to the basin. Extreme droughts depleted the lake in Helmand. Human intervention have caused the shrinking of the Aral Sea and the lakes in the lower Yangtze River. As AWT retreats and feeds lakes, we need to take immediate action for managing risks and adaption.

Plain Language Summary

Based on satellite observations, more than 80% of the lakes around Asian water towers have shown an expansion trend over the past 40 years. The expansion of these lakes is strongly linked to changes in rain, snow, glaciers and permafrost due to climate warming. As the climate continues to warm, we need to take adaptation and risk prevention measures.

1 Introduction

Lakes are both effective indicators of environmental and climate change at the basin scale because they buffer synoptic-scale changes(Grant et al., 2021; Woolway et al., 2020; Zhao et al., 2022), but also contain information on seasonal cycles, interannual variability, and long-term changes in lower atmospheric conditions(Golub et al., 2022). Studying changes in lakes under a warming climate is therefore an important area of research to distinguish the global impacts of climate change from other anthropogenic pressures of climate change interactions(Field et al., 2014).

The Asia Water Tower (AWT) region is home to numerous glaciers, lakes, and rivers that provide water for almost 2 billion people (W. W. Immerzeel et al., 2020; Yao et al., 2022) and (Yao et al., 2019). However, warming rates in AWT is twice the global average warming rate (Yan et al., 2020; You et al., 2021). Significant climate warming in AWT can cause significant hydrologic and geomorphic changes (Kim & Bae, 2020; K. E. Miles et al., 2020; Wu et al., 2022). In recent decades, lakes over the AWT have warmed, with sustained glacier mass loss (Dehecq et al., 2019; Farinotti, 2017; Lutz et al., 2014) and shorter lake freeze-up periods (Gou et al., 2017; Ruan et al., 2020). The available maps of lakes on Tibetan Plateau show that the number of lakes larger than 1 km^2 on the Tibetan Plateau has increased from 1080 in 1976 to 1424 in 2018, while the overall lake area expanded from 40124 km^2 to 5032 km^2 (G. Zhang et al., 2020). The majority of these increases in size lakes were found in endorheic basins, whereas exorheic basin lakes in the southern Tibetan Plateau and Himalayas showed a diminishing tendency (G. Zhang, Yao, Piao, et al., 2017). These changes threaten residents and infrastructures downstream since meltwater and runoff is the main water source for irrigation, hydropower, and urban consumption (Biemans et al., 2019; Walter W. Immerzeel et al., 2010; D. Li et al., 2022; Wester et al., 2019). The expansion of AWT glacial lakes will raise the risk of flooding, particularly in the eastern Himalayas, which might nearly triple in the future (Veh et al., 2019; Zheng et al., 2021). Therefore, measuring

lake size not only can be strong evidence of how climate change impacts nature but also reveal the potential crisis that can result in immeasurable ecological and social costs.

The effects of climate change on lakes may vary with geography. In some basins, streamflow would increase, and lakes would grow. In others, low runoff would occur more frequently, and severe droughts may cause lakes to shrink. (Pekel et al., 2016) mapped worldwide surface water using Landsat imagery between 1984 and 2015. It shows substantial permanent surface water loss like the Aral Sea due to uncontrolled abstraction, dams, and drought in the Middle East. However, surface water on the Tibetan Plateau has a general expansion trend. (G. Zhang, Yao, Piao, et al., 2017) found that the area of lakes on the Mongolian plateau and the eastern plains of China was decreasing. These studies show that lake systems around the AWT may not respond to climate change in the same way, and they may also respond in opposite ways to basin systems due to human intervention.

There is a lack of comprehensive and quantitative studies on how lakes located in basins recharged by the AWT, change under a warming climate. Most of the studies have been conducted from regional concepts such as the Tibetan Plateau or a country, but few have been conducted from a geologically profound concept such as the Asian Water Tower (Song et al., 2014; G. Zhang, Yao, Piao, et al., 2017). Existing studies have shown that glacial lakes in this region are becoming more and larger as a result of climate warming (Allen et al., 2019; Nie et al., 2017; Wang et al., 2020; Zheng et al., 2021). Discovering how large non-glacial lakes recharged by the AWT will respond to a warmer climate may be a challenge. In this work, we conducted a comprehensive study using 89,480 satellite images to quantify changes and identify trends in the lake over the past four decades.

2 Study Site

High-Mountains Asia, mainly the Tibetan Plateau, is known as the "Third Pole" of the world due to its numerous glaciers. Extended westward and northward from the Third Pole, the 20-million km^2 Pan-Third Pole (Pan-TPE) encompasses the Eurasian highlands and areas hydrologically affected by them: Amu Darya, Ganges, Helmand, Ili, Indus, Inner Tibetan Plateau (TP), Irrawaddy/Salween, Mekong, Syr Darya, Tarim Interior, Yangtze, and Yellow River basins. It is one of the most vulnerable and freshwater-rich regions on Earth with uncertain impacts of climate change (Tandong et al., n.d.). Figure 1 shows the range of the study site (62 °E - 120 °E and 10 °N - 51 °N).

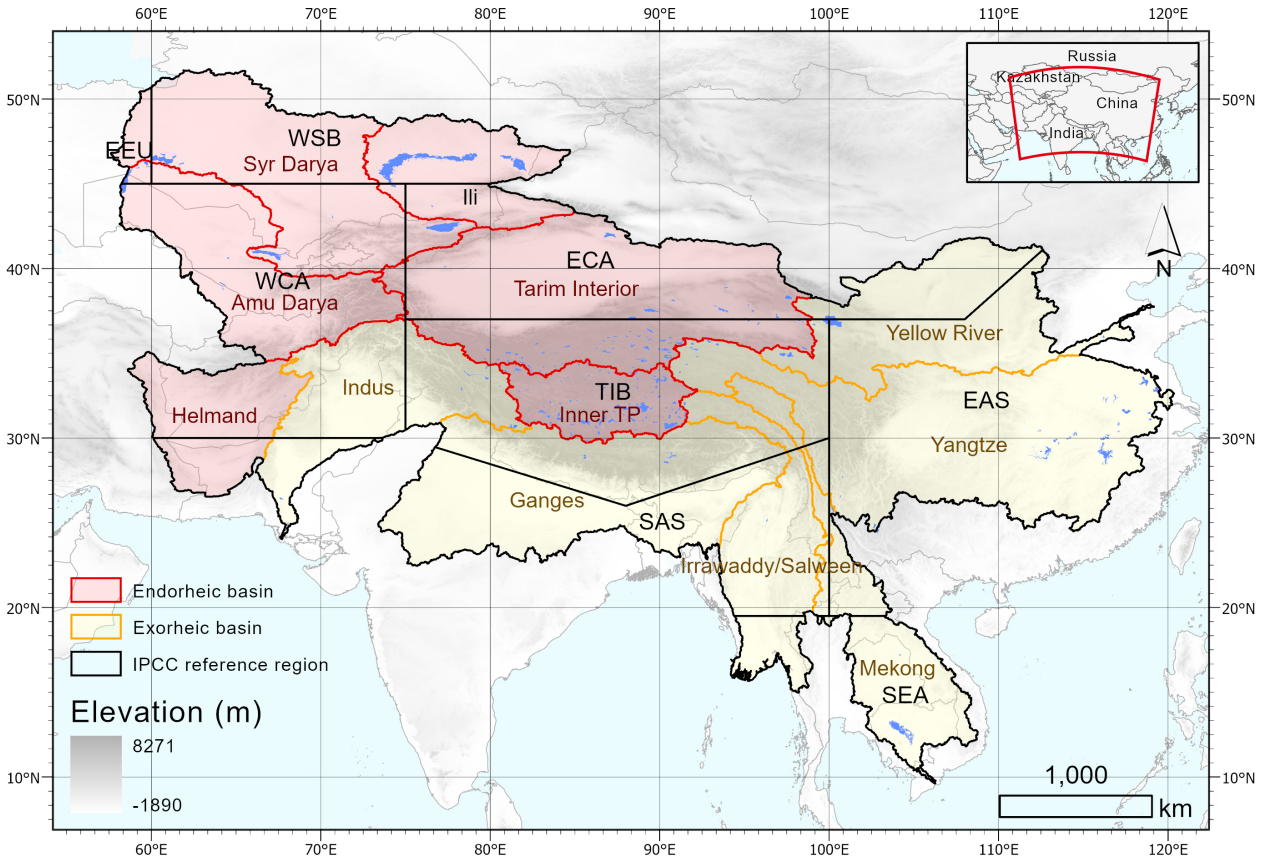

Figure 1 The basins fed by AWT. Red indicates endorheic basins, yellow indicates exorheic basins. The black lines indicate the IPCC reference region, which is used to divide the region for classification. The eight IPCC reference zones are EEU (East Europe), WSB (West Siberia), WCA (West Central Asia), ECA (East Central Asia), TIB (Tibetan Plateau), EAS (East Asia), SAS (South Asia), SEA (South East Asia).

3 Methodology

3.1 Data acquisition

3.1.1 Satellite data

To understand the changes in the lakes under a warming climate, Images from multiple Landsat sensors in five different periods from 1977 to 2020 were used. Landsat images from earlier years have insufficient coverage or poor image quality, so we produced 5-year mosaics in five periods: 1975-1979, 1988-1992, 1998-2002, 2008-2012, and 2018-2022. It has been shown that the typical five periods can reveal the overall trend of lake changes (Lei et al., 2014; G. Zhang et al., 2020). When mapping the 1977 lakes, we primarily used images from

the Landsat-2 MSS and the 1978-1979 Landsdat-3 MSS images, with a small amount of images from the Landsat-1 MSS between 1973 and 1974 and Landsat-3 MSS in 1980 used to supplement. The computed top-of-atmosphere (TOA) reflectance of Landsat-5 TM was used to map lakes from 1990±2, 2000±2, and 2010±2. We also used the Landsat-7 ETM+ for the map in 2000±2, it was not used for 2010±2 due to the data gaps. The TOA reflectance of Landsat-8 OLI was used to map lakes from 2020±2.

ALOS DEM (Digital Elevation Model) satellite data at 30-m resolution collected by Advanced Land Observing Satellite-1 (ALOS) of Japan Aerospace Exploration Agency (JAXA) was used to map the complex topography of the alpine mountain. It is useful to eliminate the effect of mountain shadows in the classification

Approximately 150,000 Landsat images were used in this study, they are accessed and analyzed online using Google Earth Engine (GEE). GEE is a cloud-based platform that enables users to process large-scale satellite imagery for detecting changes and mapping trends. Fact that we don't need to download the raw data to the local disk, the processing efficiency of the satellite images was greatly improved.

3.1.2 Vector data

We made use of two datasets from HydroSHEDS (https://www.hydrosheds.org/), HydroBASINS and HydroLAKES. HydroBASINS is a database providing the polygon layers of global basins and sub-basin boundaries. This product includes consistently sized and hierarchically nested sub-basins at different scales (from tens to millions of square kilometers). In our study, we defined basins affected by AWT using the layer of HydroBASINS level-3 product.

HydroLAKES is a database that contains the shoreline polygons of all global lakes with at least 0.1 km^2 of surface area. All lakes are co-registered with the global river network of the HydroSHEDS database via their lake pour points. HydroLAKES enabled us to distinguish 'natural lakes' from 'human-made reservoirs', it also served as the public dataset for accuracy validation of our work.

3.1.3 Climatic data

Four climate datasets including ERA-5 Land, TerraClimate (Abatzoglou et al., 2018), FLDAS (McNally et al., 2017), and GPM were used in this study. Monthly precipitation and snow water equivalent are provided by ERA-5 Land, TerraClimate, and FLDAS. GPM dataset only provides the precipitation data. These data were accessed and processed on the GEE platform like the satellite data to help us analyze the causes of Pan-third Pole lake expansion.

As for glacier mass loss, Brun et al., 2017; Shean et al., 2020 estimated the glacier mass balance per year for each basin, so we can estimate the glacier mass loss from 2000 to 2020. As for permafrost, we estimated the permafrost active layer thickness from 2000 to 2019 for each basin according to the Permafrost active layer thickness for the Northern Hemisphere dataset of European Space Agency

(ESA)'s Climate Research Data Package (CRDP v2). All data used in this study are shown in Table 1.

Table 1. Summary of the datasets used in the study.

Data type	Name	Spatial resolution (meters)	Temporal resolution	Use	Source
Satellite data	Landsat-1/2/3 MSS		days	Mapping lakes	GEE: LANDSAT/LC08/C01/T1_TOA LANDSAT/LE07/C01/T1_TOA LANDSAT/LT05/C01/T1_TOA LANDSAT/LM03/C01/T2 LANDSAT/LM02/C01/T2 LANDSAT/LM01/C01/T2 JAXA/ALOS/AW3D30/V3_2
	Landsat-5 TM		days		
	Landsat-7 ETM+		days		
	Landsat-8 OLI		days		
	ALOS DEM		\	Eliminate the effect of mountain shadows in the classification	
Vector data	HydroBASINS	\	\	Delineate the basins	HydroSHEDS (https://www.hydrosheds.org/)
	HydroLAKES	\	\	Define the natural lakes, and assess the accuracy of our maps in 2000	
Climatic data	ERA-5 Land		Monthly	Analysis of precipitation and snow water equivalent	GEE: ECMWF/ERA5_LAND/MONTHLY IDAHO_EPSCOR/TERRACLIMATE NASA/FLDAS/NOAH01/C/GL/M/V00 NASA/GPM_L3/IMERG_MONTHLY_
	TerraClimate		Monthly		

Data type	Name	Spatial resolution (meters)	Temporal resolution	Use	Source
	FLDAS		Monthly		
	GPM		Monthly	Analysis of precipitation	
	Potential contribution of glaciers to basins		-2016	Analysis of glaciers	Brun et al., 2017; Shean et al., 2020
	Permafrost active layer thickness for the Northern Hemisphere		Yearly 1997-2019	Analysis of permafrost	https://catalogue.ceda.ac.uk/uuid/67a3f8c8dc914ef99f7f08eb0d997e23

3.2 Data acquisition

3.2.1 Mapping lakes

The study area is large and covers different climatic systems and terrain, which can affect the classification effect of the lakes. We used IPCC climate reference regions (Iturbide et al., 2020) to divide the study area into six parts (Figure 1). Among them, we merged WCA, WSB, and EEU for classification because the Aral Sea crosses WCA and WSB, and EEU is a very small extent in the study area.

Most of these basins are under monsoon systems and the recharge of the lakes can vary depending on the season. Therefore, we analyzed satellite images collected in the wet season and the dry season separately in each period. For the EAS, TIB, ECA, and WCA/WSB/EEU, which are located in the north temperate zone, the wet season starts from June to September, and the dry season starts from December to March (Azam et al., 2021; Y. Zhang et al., 2020). Due to the high latitude of the ECA and WCA/WSB/EEU, ice on the lake surface can make it difficult to be distinguished. We removed some images of the lake surface that were difficult to identify and supplemented them with images from October and November. For the ECA and WCA/WSB/EEU lakes, October is already in the dry season (Ginzburg et al., 2010; Panyushkina et al., 2018). SEA and SAS are located in the tropics, their wet season starts from August to November, and the dry season starts from February to May (Anh et al., 2019; Kummu et al., 2014).

First, we obtained Landsat images from the GEE using date and boundary filters. Since each basin has unique topographical and climatic circumstances, we worked to classify each one independently. Then, we masked cloudy pixels from images by examining the internal cloud-algorithm-flag bits, and mosaic all the images by creating a median mosaic. To highlight the water pixel and to distinguish it from the surface snow, we derived two normalized indices: Normalized Difference Water Index (NDWI; Eq. (1)) (McFEETERS, 1996) and Normalized Difference Snow Index (NDSI; Eq. (2)). NDWI is sensitive to the change in the water content. NDSI is an accurate description of snow detection. Mountain shading is one of the most obvious interferences in the classification of water bodies. The slope calculated by ALOS DEM can reduce the possible shading effect (Shugar et al., 2020).

$$\text{NDWI} = \frac{GREEN-NIR}{GREEM+NIR} \quad (1)$$

$$\text{NDWI} = \frac{GREEN-SWIR1}{GREEN+SWIR1} \quad (2)$$

Consequently, Blue, Green, Red, Near-Infrared, Mid-infrared bands, NDSI, NDWI, and slope were used to classify water and non-water pixels on the Landsat 5-8 images (Green, Red, Near-Infrared 1, and Near-Infrared 1 were used on the Landsat 1-3 images). We randomly selected water and non-water samples by drawing polygons using the drawing tool in GEE. To avoid reselecting samples in each classification, we selected pixel points that are consistent over the five periods. Then, we randomly converted the polygon samples into 5000 points. We had 5000 sample points in total, and we split 80% of the points for training and 20% for testing. We then conducted a classification using Support Vector Machine (SVM) classifier with default parameters. The classification results (binary) images were exported to ArcGIS Pro and vectorized. We first removed the non-water feature and then calculated the area of the remaining features. In our study, we only kept natural lakes larger than 50 km^2 in 2020. The HydroLAKES dataset can help filter artificial reservoirs.

The remaining 20% samples were used for validation, which was 1000 points. The accuracy of our results is shown by Confusion Matrix, overall accuracy, user accuracy, producer accuracy, Kappa coefficient, and R^2. We also validated our results by randomly selecting 10 thousand points from our results and comparing them with public datasets: i) HydroLAKES (Messager et al., 2016), and ii) Lakes Larger than 1 km^2 from the Tibetan Plateau V3.0 (G. Zhang et al., 2014, 2019). Because lake shorelines of HydroLAKES were delineated as they appeared at the time of the data collection in February 2000, we used this dataset to validate our year 2000 results. All other periods were compared with the dataset of Lakes Larger than 1 km^2 in Tibetan Plateau V3.0. Both datasets do not fully cover the temporal and spatial extent of our maps, and validating the accuracy of our results together can better illustrate the accuracy of the results. The accuracy of each classification for each basin was validated. All of these results have a kappa coefficient greater than 0.95 and R^2 over 0.90.

3.2.1 Driving forces analysis

Zhang et al., 2017b showed that lake water mass balance is mainly due to changes in precipitation, snow, glaciers, and permafrost in the basin. Using GEE, we constructed a sum mosaic for calculating the total annual precipitation and total annual snow water equivalent for each basin from these four climatic datasets. To improve the accuracy as much as possible, we used the average of total annual precipitation of the four datasets. Since the GPM contains only precipitation, we only used the average snow water equivalent from the three datasets ERA-5 Land, TerraClimate, and FLDAS. As a result, the average yearly change rate of total annual precipitation and total annual snow water equivalent was obtained.

Based on results from Brun et al., 2017; Shean et al., 2020, we can directly obtain the average annual rate of change in glacier mass change for each basin. As for permafrost, we downloaded the CRDP v2 permafrost active layer thickness data from 2000 to 2019, and converted these data into a single '.tif' file with 20 layers stacking, the layers indicate the year of the image. To make our results more easily reproducible, we uploaded them to GEE for further processing.

4 Results

4.1 Lake changes

From 1977±2 to 1990±2, most of the alpine lakes showed a shrinking in size trend, while the plain lakes showed an expanding trend during the wet season (Fig.2). From 1990 to 2000, shrinkage of alpine lakes slowed, and some of them were starting to expand. Most of the eastern and western Plains lakes had a declining tendency, the plains lakes in the north and south are still expanding. From 2000 to 2010, most of the alpine lakes and some of the western plain lakes have expanded, whereas the plain of the Yangtze basin continued to shrink. From 2010 to 2020, the alpine lakes were still expanding, with only few were shrinking. Most of the plain lakes were shrinking.

Comparing the lake size from 1977±2 to the lake size from 2020±2, 84% have grown in size while 16% lakes have diminished. In terms of area, the total lake expansion is 13,048km^2 while the total lake shrinkage is 50,896km^2. The shrinking area is more than the expanding area, but 90% of the total shrinking area is due to the Aral Sea. The shrinking lakes are primarily located in the basins downstream of Helmand and Yangtze.

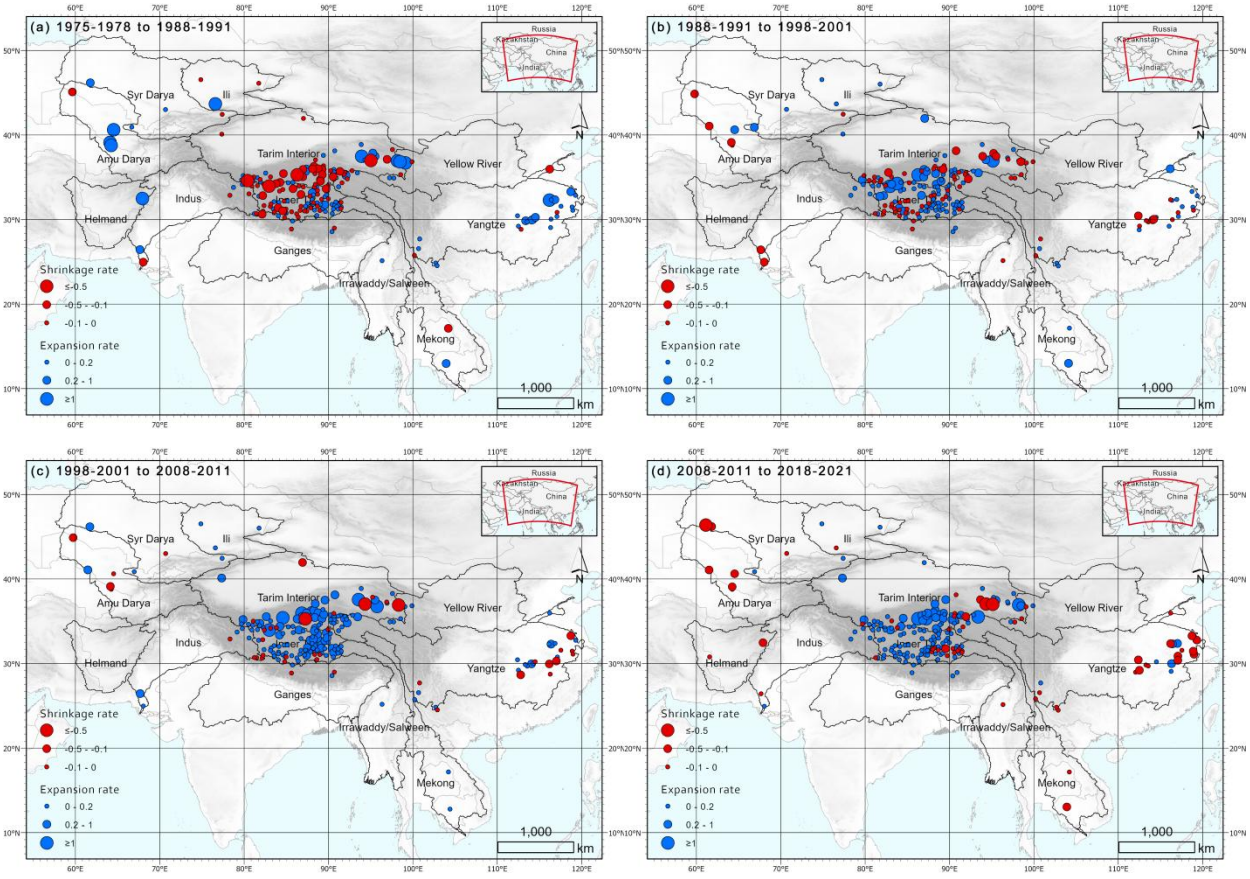
(a) 1975-1978 to 1988-1991
(b) 1988-1991 to 1998-2001
(c) 1998-2001 to 2008-2011
(d) 2008-2011 to 2018-2021
Russia
Kazakhstan
China
India
Syr Darya
Ili
Amu Darya
Tarim Interior
Yellow River
Indus
Inner
Helmand
Yangtze
Ganges
Irrawaddy/Salween
Mekong
Shrinkage rate
≤-0.5
-0.5 - -0.1
-0.1 - 0
Expansion rate
0 - 0.2
0.2 - 1
≥1
1,000
km
N

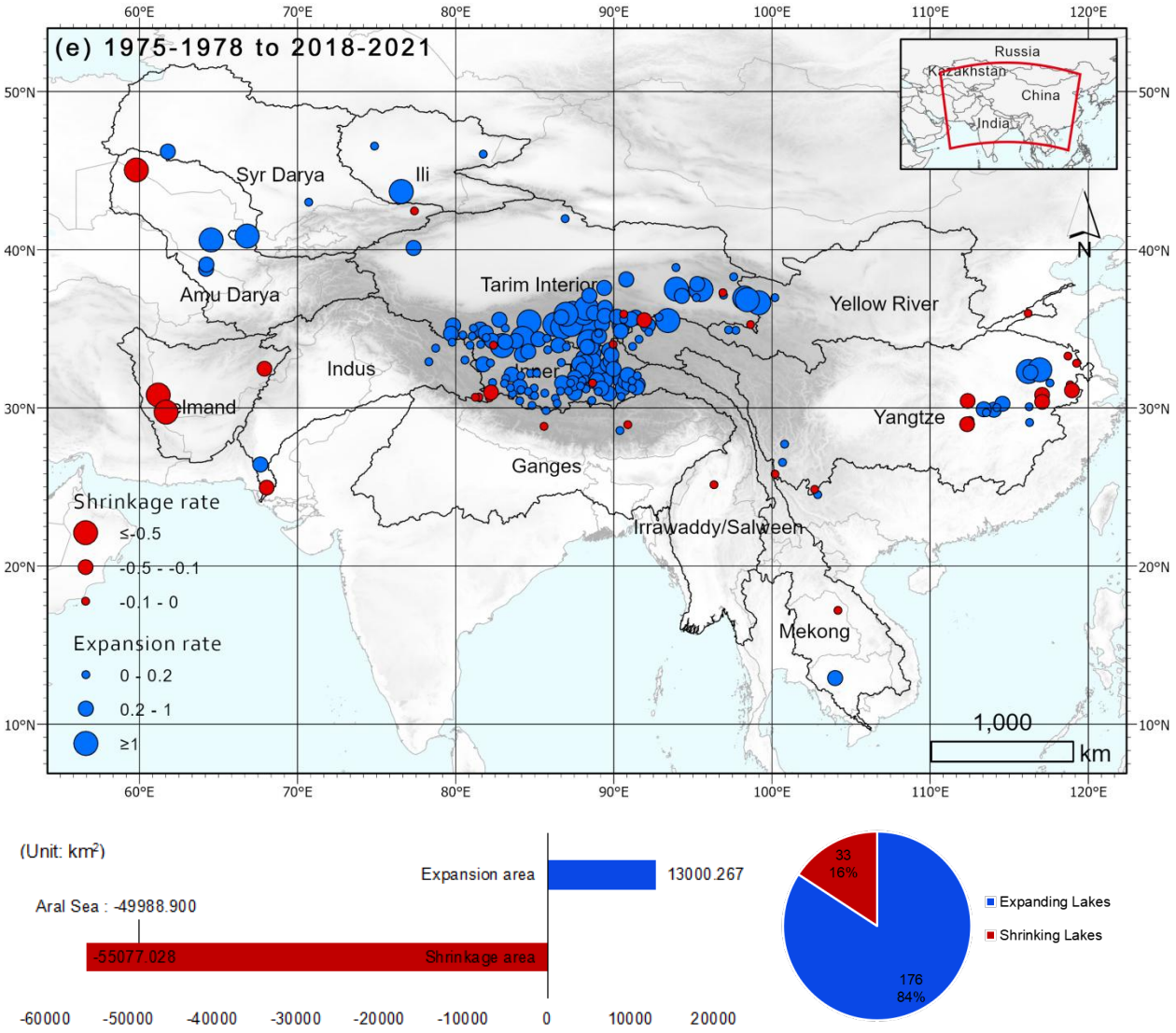

Figure 2 Lake change in the (a), wet season from 1977±2 to 1990±2 (b), wet season from 1990±2 to 2000±2 (c), wet season from 2000±2 to 2010±2 (d), wet season from 2010±2 to 2020±2 (e), wet season from 1977±2 to 2020±2

The spatio-temporal pattern of lake size in the dry season is generally consistent with that in the wet season (Fig.3). In the dry season from 1977±2 to 2020±2, 170 lakes have grown in size, while 39 lakes have declined. A small number of lake variations show seasonal variances between dry and wet. The sum of the lake area growth is 11,244km^2, and the sum of the lake area shrinkage is 51,587km^2. The shrinking area of the Aral Sea still accounts for the majority of the total shrinking area.

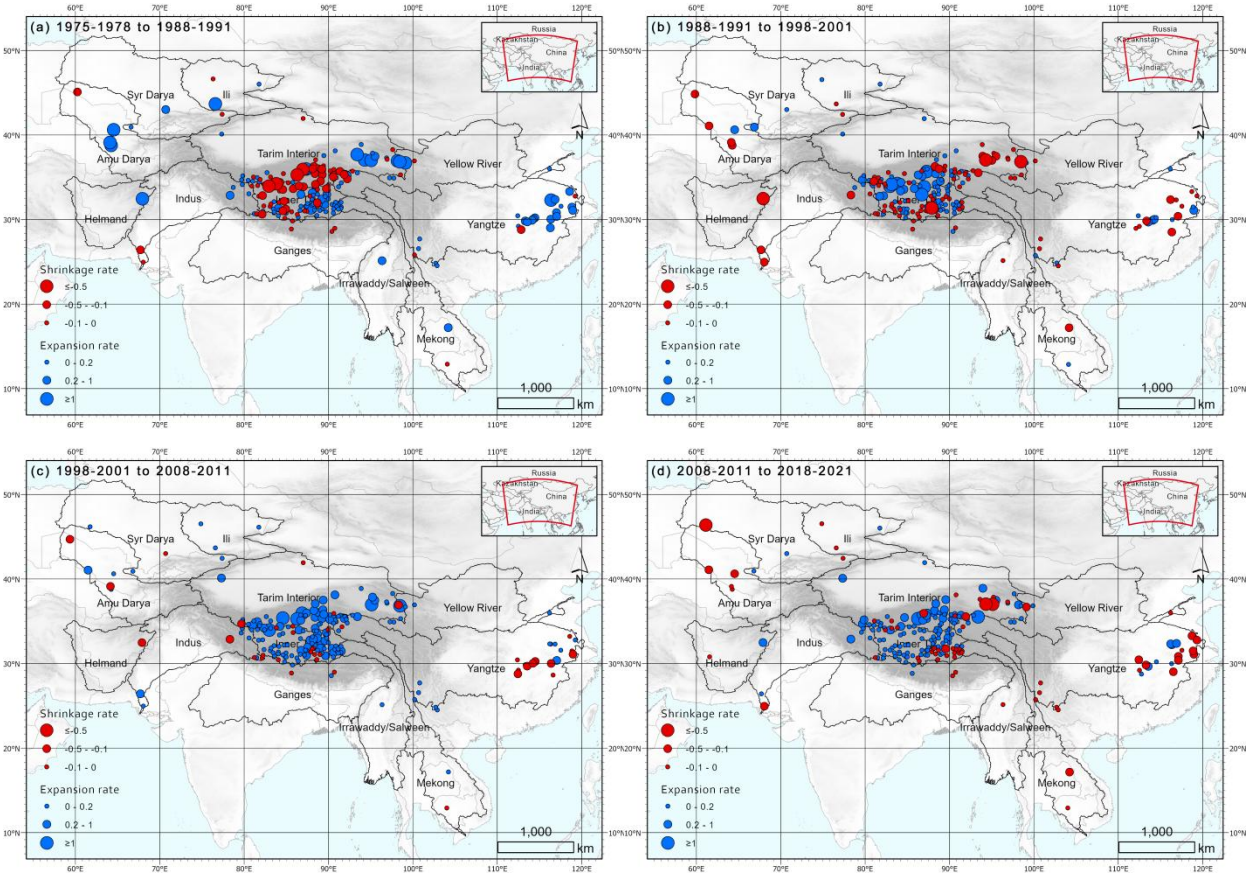
(a) 1975-1978 to 1988-1991
(b) 1988-1991 to 1998-2001
(c) 1998-2001 to 2008-2011
(d) 2008-2011 to 2018-2021
Syr Darya
Ili
Amu Darya
Tarim Interior
Yellow River
Indus
Helmand
Yangtze
Ganges
Irrawaddy/Salween
Mekong
Shrinkage rate
≤-0.5
-0.5 - -0.1
-0.1 - 0
Expansion rate
0 - 0.2
0.2 - 1
≥1
1,000
km
N
Russia
Kazakhstan
China
India

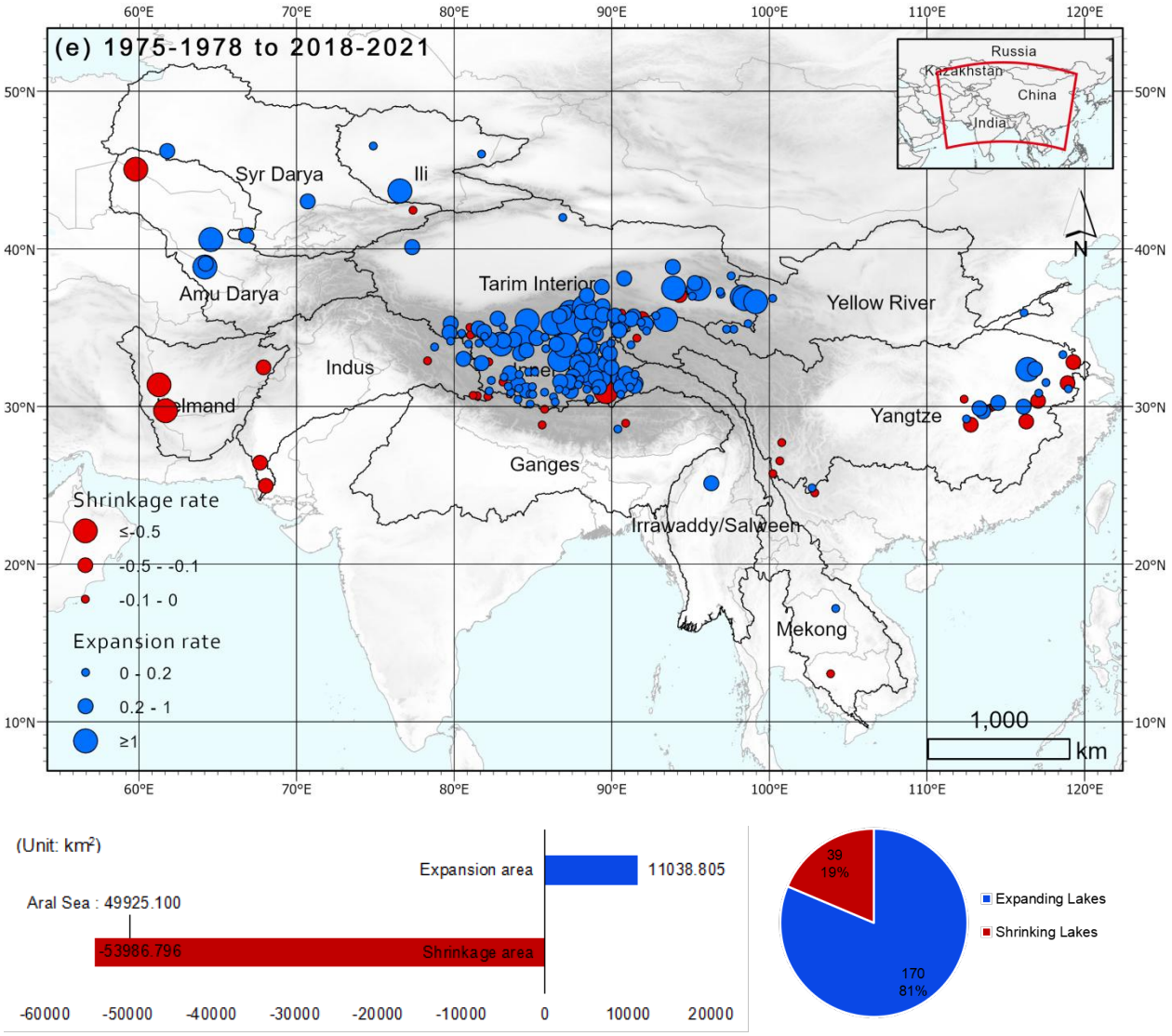

Figure 3 Lake change in the (a), dry season from 1977±2 to 1990±2 (b), dry season from 1990±2 to 2000±2 (c), dry season from 2000±2 to 2010±2 (d), dry season from 2010±2 to 2020±2 (e), dry season from 1977±2 to 2020±2

4.3 Water basin analysis

In the wet season from 1977±2 to 2020±2 (Figure 4), the total lake area in the Inner TP, Tarim Interior, Syr Darya, and Mekong basins was growing at rates of 64.095 (0.43%), 106.650 (1.14%), 44.408 (2.35%), and 82.28 (1.95%) km^2 yr^{-1}, respectively. But the total lake area in the Mekong basin decreased in 2020. The lakes in the Amu Darya, Helmand, and Ganges basins were shrinking

at rates of -1141.9 (1.97%), -108.870 (2.56%), and -0.686 (0.05%) km^2 yr^{-1}, respectively. From 1977±2 to 2000±2, the total lake area in the Yangtze basin increased but then declined from 2000±2 to 2020±2. Lakes in the Yellow River, Irrawaddy/Salween, Indus, and Ili basins were with no significant trends.

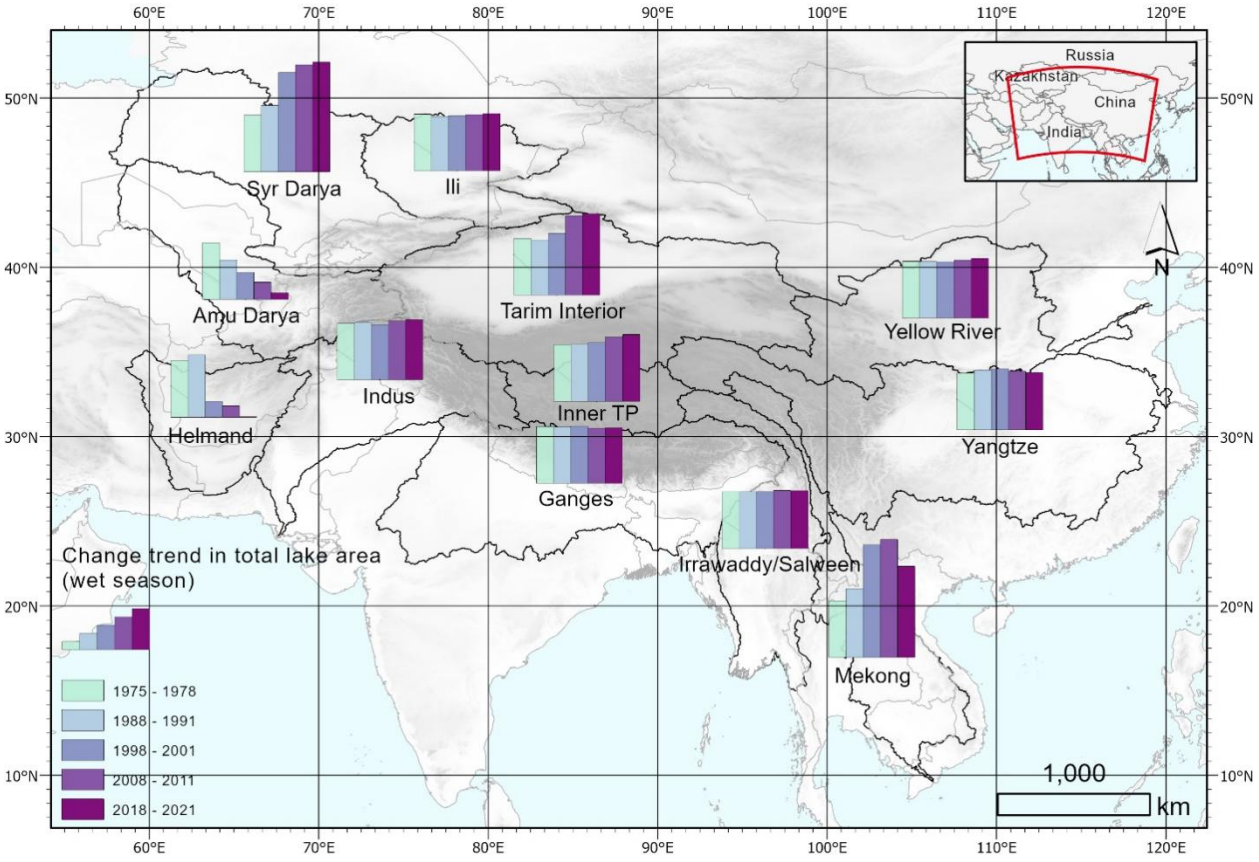

Figure 4 Total lake area change in each basin during the wet season from 1977±2 to 2020±2.

In the dry season from 1977±2 to 2020±2 (Figure 5), the lakes in Inner TP, Tarim Interior, and Syr Darya basins also showed a trend of expansion with growth rates of 94.579 (0.41%), 61.105 (1.04%), and 42.925 (2.21%) km^2 yr^{-1}, respectively. However, the total lake area in the Mekong basin decreased in the dry season, contrary to the trend in the wet season, with a rate of decrease of 3.998 km^2 yr^{-1}. The lakes in the Amu Darya, Helmand, and Ganges basins still showed a shrinking trend in the dry season, with a rate of decrease of 1091.7 (1.94%), 60.528 (2.52%), and -1.255 (0.1%) km^2 yr^{-1}, respectively. The total lake area in the Yangtze Basin still showed an increasing trend followed by a decreasing trend, but it showed an increasing trend from 1977±2 to 1990±2 and a decreasing trend after 1990±2, and lakes in the Yellow River,

Irrawaddy/Salween, Indus, and Ili basins remained stable during the dry season with no significant trends.

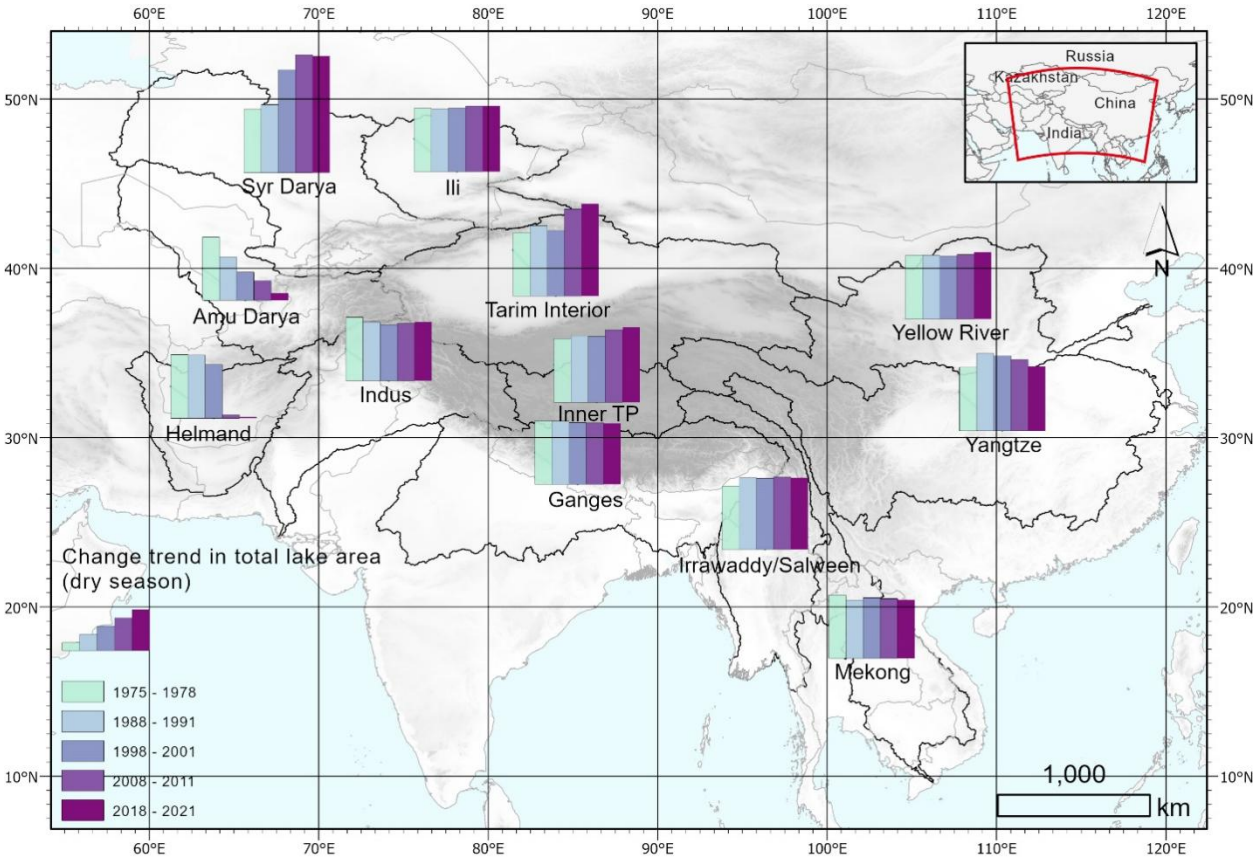

Figure 5 Total lake area change in each basin during the dry season from 1977±2 to 2020±2.

4.4 Driving forces

We estimated the annual average change rates from 2000 to 2020 for the three potential sources of lake recharge: precipitation, snow water equivalent, and glacier mass loss (Fig. 4). If the value is positive, it means that it has a positive contribution to the recharge of the basin. Snow water equivalent in the Amu Darya was rapidly dropping, while precipitation and glacier mass loss were rising. All three water sources in the Ganges were moving toward a growing trend and the snow water equivalent was rising significantly, but the lake in the Ganges was not growing much. In Helmand, precipitation and snow water equivalent were increasing, but there is no glacial recharge. In Ili, Inner TP, Irrawaddy/Salween, Mekong, and Syr Darya basins, only the loss of glacial mass was growing, while their precipitation and snow water equivalent were

decreasing. In Irrawaddy/Salween and Mekong, the decline in precipitation was particularly significant. There was a dramatic increase in precipitation in the Yangtze and Yellow River basins, but the lakes did not respond to it. Both basins have large populations, which leads to changes in the lakes that are influenced by human activities. For the Inner TP and Syr Darya, the increase in the lake area is mainly due to the loss of glaciers. In the Tarim Interior basin, precipitation and snow water equivalent correspond to the trend of lake growth. The expansion of the lake area in the Indus basin should be driven primarily by precipitation, but snow and glaciers also played a role.

[CHART]

Figure 6 Average annual change rate of total precipitation, snow depth water equivalent, and glacier mass loss from 2000 to 2020 for each basin. Orange indicates precipitation, blue indicates snow water equivalent, and gray indicates glacier mass loss.

Permafrost degradation also plays an important role in driving changes in these lakes. We found that the active layer thickness of permafrost in all the basins tend to increase between 2000 and 2020 based on ESA's Northern Hemisphere permafrost data, suggesting a gradual thawing of permafrost (Figure 7). In the continuous permafrost areas, lakes expand in size and increase in number, while in discontinuous, sporadic, and isolated permafrost areas, lakes decline in size and decrease in number (Smith et al., 2005). Li et al., (2014) found that the distribution of high Asian permafrost is consistent with lake change patterns. The expanding highland lakes are due to the melting of continuous permafrost, especially in the southern highlands of the Tarim Interior, whose cooler temperatures result in a continuous increase in permafrost contribution to lake expansion without a slowing trend. The area with shrinking lakes in the south of Inner TP, western of Indus, the northern of Ganges, and Helmand Basins is part of an isolated permafrost zone. This may also account for the changes in shrinking lakes in Indus and Ganges basin although rainfall, snow, and glaciers have all contributed significantly to them, and the Helmand Basin has shown an increasing trend in rainfall and snow water equivalent despite the absence of glacial recharge.

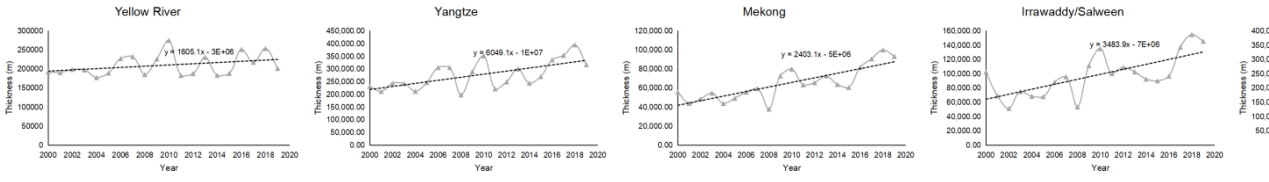

Figure 7 Trend of permafrost active layer thickness from 2000 to 2019 for each basin.

5 Discussion

Our result shows a consistent trend relative to the findings from the published

studies. (Lei et al., 2014; G. Zhang et al., 2014, p. 20) used Landsat TM/ETM+ data to show that the area of Inner TP lakes increased at a rapid rate (~27%) between the 1990s and 2010. (Wan et al., 2016) used the China-Brazil Earth Resources Satellite (CBERS) (2005) and China's newly launched GaoFen-1 (GF-1) to map the lakes in Tibetan Plateau and found that the lakes in Inner TP have been expanding from 2005 to 214 at an average growth rate of 9.88%. Zheng et al. 2019 used Landsat imagery to map 959 lakes in the Syr Darya and found that their average relative growth rate from 1990 to 2015 was 94%. (Shi et al., n.d.) based on Advanced Very High Resolution Radiometer (AVHRR) satellite observations showed a continuous shrinkage of the Aral Sea from 1981-2013. (Tayfur & Alami, 2022) found that Helmand experienced extreme dry weather in the summer of 2001, which explains the Helmand watershed had a smaller lake area in the wet season in 2000 than in the dry season. These existing conclusions further illustrate the reliability of our results. But changes in the area may not reflect the same level of changes in water volume, expansion is not always visible, especially in deep lakes. It is very challenging to find a time-series bathymetric dataset that covered the entire time frame of the study. We will reveal the water volume changes in these lakes in further studies.

In assessing the drivers of lake change, we only considered the recharge source changes from 2000 to 2020 as a reference due to the lack of available glacier data. According to our lake size change maps, the period from 2000 to 2020 is also the period with the most pronounced lake expansion trend. (G. Zhang, Yao, Shum, et al., 2017) estimated the water storage change in Inner TP using Gravity Recovery and Climate Experiment (GRACE) satellite data, and found the precipitation contributed to the majority (74%) of the increase in lake water storage, followed by glacier melting (13%) between 2003 and 2009. However, in our study, we found a decreasing trend of rainfall in Inner TP from 2000 to 2020. All four data (ERA-5, TerraClimate, FLDAS, and GPM) that we used to estimate rainfall show a decreasing trend in rainfall in Inner TP during this period. We would not deny that all four precipitation datasets may have errors, and we analyzed a longer time range, which may also lead to different results. Our investigation and (G. Zhang, Yao, Shum, et al., 2017) both estimated the proportion of these contributors on the basin scale, which does not fully account for the true cause of the expansion of individual lakes. In further studies, remote sensing observations can be combined with in-suited measurement to further reveal the sources of lake expansion.

While climate change can significantly affect lake recharge, we should not ignore the impact of human intervention on lake change. In the Amu Darya, only the Aral Sea shows a dramatically decreasing trend, other lakes located in the upper reaches show a trend of expansion, Lake Vpadina Ayakalytma with an expansion of 4.58 times. Lake Umar and Lake Dengizkul expanded by 79.10% and 72.19%, respectively. But the Aral Sea downstream of the basin was diminishing so rapidly. According to the findings of (Micklin, 2016; Yang et al., 2020), human use of the Aral Sea is unsustainable, with excessive irrigation withdrawals and periodic diversions of the Amu Dar'ya westward contributing to its massive

shrinkage. The human intervention also occurred in the lower Yangtze basin, the most populated region. We estimated the residential population in each basin and within the 20 km buffer zone of each lake using WorldPop Global Project Population Data. The Yangtze Basin has the largest population, with its total population growing from 16.27 million in 2000 to 220 million by 2020. The population around Dongting Lake, which has the largest shrinking area, grew from 8.27 million in 2000 to 9.68 million in 2020, and it is also the lake with the largest population living around it.

Under the influence of climate change, most of the lakes recharged by AWT were expanding. However, this pattern of expansion will not continue indefinitely. Because the recharge from the snow, glaciers, and permafrost would not always increase in the future. Wang et al. 2018 found that the global endorheic system experienced a widespread water loss of approximately 106.3 Gt yr^{-1} during 2002-2016. The glacier mass loss rate for the entire AWT during 2000-2016 is 16.3±3.5 Gt yr^{-1} (Brun et al., 2017). In the future, the Asian meltwater supply is likely to decrease dramatically (Kraaijenbrink et al., 2021). The ablation of AWT glaciers is mostly unsustainable, and the seasonality of total river runoff, glacier melt and flow is expected to increase and then decline by 2050 (Azam et al., 2021). AWT glacier ablation into rivers will be reduced by 28% ± 1% by 2100 (E. Miles et al., 2021). Moreover, 37.3% of the permafrost on the Tibetan Plateau is at risk of disappearing, and it is expected that under the RCP8.5 scenario, the permafrost area will be reduced to 42% of the current area (Ni et al., 2021). In the face of the threat that AWT warming poses to our freshwater resources, we need to take action immediately to adapt to these changes and prevent further deterioration.

6 Conclusions

Based on Landsat images, the boundaries of 209 Asian water towers' lakes in the dry and wet seasons from 1997±2, 1990±2, 2000±2, 2010±2, and 2020±2 were mapped in this study. These maps show good accuracy with kappa coefficients over 0.95 and R^2 over 0.9. Our maps show that most upstream lakes shrunk, while plain lakes grew during 1977±2-1990±2. From 1990±2 to 2000±2, some alpine lake sizes were reduced while inner TP lakes expanded. Most eastern and western plain lakes were shrinking, whereas northern and southern lakes were growing. Most alpine lakes and some western plain lakes grew from 2000±2 to 2010±2, whereas the plain lakes in the Yangtze basin shrunk. Alpine lakes still expanded and plain lakes shrunk from 2010±2 to 2020±2. Overall, from 1977±2 to 2020±2, although the total area of shrinkage (55077.028 km^2 in wet season, 49929km^2 in dry season) is more than the area of expansion (13000.267 km^2 in wet season, 11038.805 in dry season), this is mainly due to the Aral Sea's shrinkage, it accounts for 90% of the total shrinkage area. The number of expanding lakes (176, 84% in the wet season; 170, 81% in the dry season) is significantly more than the number of shrinking lakes (33, 16% in the wet season; 39, 19% in the dry season).

From a basin perspective, the expanding lakes are mainly located in the Inner

TP and Tarim Interior basins. The total lake area in Inner TP, Tarim Interior, Syr Darya, and Mekong basins shows an overall increasing trend in the wet season with growth rates of 106.650, 44.408, and 82.28 km^2 yr^{-1}, respectively. In the dry season, the Mekong basin shows the opposite trend (shrunk at a rate of -3.998 km^2 yr^{-1}), while the lakes in the other three basins still expand (grew at rates of 64.095, 106.650, 44.408, and 82.28 km^2 yr^{-1}). The total lake area in the Amu Darya, Helmand, and Ganges basins show a decreasing trend in both the wet and dry seasons (The shrinkage rates in the wet season were -1141.900, -108.870, and -0.686 km^2 yr^{-1}, respectively. The shrinkage rates in the dry season were -1091.700, -60.528, and -1.255 km^2 yr^{-1}, respectively.), while the total lake area in the Yangtze basin still shows an increasing trend followed by a decreasing trend. The total lake area in the Yellow River, Irrawaddy/Salween, Indus, and Ili basins was stable in both wet and dry seasons with no significant trend.

The lake expansion in the Inner TP, Tarim Interior, Syr Darya, and Mekong basins is related to the glacial loss. Lake shrinkage in the Yangtze and the dramatic loss of the Aral Sea are primarily due to human intervention. The expansion of other Amu Darya lakes is corresponding to the trend of precipitation and glaciers. Permafrost thawing also contributed to the expansion of these lakes. Due to permafrost discontinuities, increased recharge in the Indus and Ganges basins but no significant expansion of lakes may be the result. The regular occurrence of drought events is the main cause of the Helmand basin lakes' depletion after 2000.

Acknowledgments

Nuo Xu conceived and conducted most of the study, analyzed a large amount of data, and wrote the manuscript. Andre Daccache provided extensive technical guidance. Peng Gou proposed and designed the study. All authors edited the manuscript and responded to comments. This work was supported by the Big Data Technology Research Center of Nanhu Laboratory and the National Natural Science Foundation of China (42130306).

Open Research

Data availability

The complete lakes database is available at https://github.com/samapriya/awesome-gee-community-datasets/issues/57

Code availability

For 1990±2, 2000±2, 2010±2, 2020±2:

https://code.earthengine.google.com/bab27dc1f3d7db7b6b83802331c82e6d

For 1977±2:

https://code.earthengine.google.com/00ca8d0e2bcc578fce1458c03351ca40

The basin name and date can be replaced. The accuracy indicators including user accuracy, total accuracy, Kappa coefficient, and R2 are shown on the right console.

Using ERA-5 Land, TerraClimate, FLDAS, and GPM datasets to analyze the change in annual total precipitation and snow depth water equivalent for each basin

https://code.earthengine.google.com/e195b3a9108d6656861e1202bd5a847a

Using data of Permafrost active layer thickness for the Northern Hemisphere from ESA to analyze the change of annual total thickness for each basin

https://code.earthengine.google.com/60f327a1cd32af0ca1c5fbb5e59246eb

References

Abatzoglou, J. T., Dobrowski, S. Z., Parks, S. A., & Hegewisch, K. C. (2018). TerraClimate, a high-resolution global dataset of monthly climate and climatic water balance from 1958–2015. *Scientific Data*, *5*(1), 170191. https://doi.org/10.1038/sdata.2017.191Allen, S. K., Zhang, G., Wang, W., Yao, T., & Bolch, T. (2019). Potentially dangerous glacial lakes across the Tibetan Plateau revealed using a large-scale automated assessment approach. *Science Bulletin*, *64*(7), 435–445. https://doi.org/10.1016/j.scib.2019.03.011Anh, D. T., Hoang, L. P., Bui, M. D., & Rutschmann, P. (2019). Modelling seasonal flows alteration in the Vietnamese Mekong Delta under upstream discharge changes, rainfall changes and sea level rise. *International Journal of River Basin Management*, *17*(4), 435–449. https://doi.org/10.1080/15715124.2018.1505735Azam, Mohd. F., Kargel, J. S., Shea, J. M., Nepal, S., Haritashya, U. K., Srivastava, S., et al. (2021). Glaciohydrology of the Himalaya-Karakoram. *Science*, *373*(6557), eabf3668. https://doi.org/10.1126/science.abf3668Biemans, H., Siderius, C., Lutz, A. F., Nepal, S., Ahmad, B., Hassan, T., et al. (2019). Importance of snow and glacier meltwater for agriculture on the Indo-Gangetic Plain. *Nature Sustainability*, *2*(7), 594–601. https://doi.org/10.1038/s41893-019-0305-3Brun, F., Berthier, E., Wagnon, P., Kääb, A., & Treichler, D. (2017). A spatially resolved estimate of High Mountain Asia glacier mass balances from 2000 to 2016. *Nature Geoscience*, *10*(9), 668–673. https://doi.org/10.1038/ngeo2999Dehecq, A., Gourmelen, N., Gardner, A. S., Brun, F., Goldberg, D., Nienow, P. W., et al. (2019). Twenty-first century glacier slowdown driven by mass loss in High Mountain Asia. *Nature Geoscience*, *12*(1), 22–27. https://doi.org/10.1038/s41561-018-0271-9Farinotti, D. (2017). Cryospheric science: Asia's glacier changes. *Nature Geoscience*. https://doi.org/10.1038/ngeo.2995Field, C. B., Barros, V. R., Dokken, D. J., Mach, K. J., & Mastrandrea, M. D. (Eds.). (2014). Terrestrial and Inland Water Systems. In *Climate Change 2014 Impacts, Adaptation, and Vulnerability* (pp. 271–360). Cambridge: Cambridge University Press. https://doi.org/10.1017/CBO9781107415379.009Ginzburg, A. I., Kostianoy, A. G., Sheremet, N. A., & Kravtsova, V. I. (2010). Satellite

Monitoring of the Aral Sea Region. In A. G. Kostianoy & A. N. Kosarev (Eds.), *The Aral Sea Environment* (Vol. 7, pp. 147–179). Berlin, Heidelberg: Springer Berlin Heidelberg. https://doi.org/10.1007/698_2009_15Golub, M., Thiery, W., Marcé, R., Pierson, D., Vanderkelen, I., Mercado-Bettin, D., et al. (2022). A framework for ensemble modelling of climate change impacts on lakes worldwide: the ISIMIP Lake Sector. *Geoscientific Model Development*, *15*(11), 4597–4623. https://doi.org/10.5194/gmd-15-4597-2022Gou, P., Ye, Q., Che, T., Feng, Q., Ding, B., Lin, C., & Zong, J. (2017). Lake ice phenology of Nam Co, Central Tibetan Plateau, China, derived from multiple MODIS data products. *Journal of Great Lakes Research*, *43*(6), 989–998. https://doi.org/10.1016/j.jglr.2017.08.011Grant, L., Vanderkelen, I., Gudmundsson, L., Tan, Z., Perroud, M., Stepanenko, V. M., et al. (2021). Attribution of global lake systems change to anthropogenic forcing. *Nature Geoscience*, *14*(11), 849–854. https://doi.org/10.1038/s41561-021-00833-xImmerzeel, W. W., Lutz, A. F., Andrade, M., Bahl, A., Biemans, H., Bolch, T., et al. (2020). Importance and vulnerability of the world's water towers. *Nature*, *577*(7790), 364–369. https://doi.org/10.1038/s41586-019-1822-yImmerzeel, Walter W., van Beek, L. P. H., & Bierkens, M. F. P. (2010). Climate Change Will Affect the Asian Water Towers. *Science*, *328*(5984), 1382–1385. https://doi.org/10.1126/science.1183188Iturbide, M., Gutiérrez, J. M., Alves, L. M., Bedia, J., Cerezo-Mota, R., Cimadevilla, E., et al. (2020). An update of IPCC climate reference regions for subcontinental analysis of climate model data: definition and aggregated datasets. *Earth System Science Data*, *12*(4), 2959–2970. https://doi.org/10.5194/essd-12-2959-2020Kim, J.-B., & Bae, D.-H. (2020). Intensification characteristics of hydroclimatic extremes in the Asian monsoon region under 1.5 and 2.0 °C of global warming. *Hydrology and Earth System Sciences*, *24*(12), 5799–5820. https://doi.org/10.5194/hess-24-5799-2020Kraaijenbrink, P. D. A., Stigter, E. E., Yao, T., & Immerzeel, W. W. (2021). Climate change decisive for Asia's snow meltwater supply. *Nature Climate Change*, *11*(7), 591–597. https://doi.org/10.1038/s41558-021-01074-xKummu, M., Tes, S., Yin, S., Adamson, P., Józsa, J., Koponen, J., et al. (2014). Water balance analysis for the Tonle Sap Lake-floodplain system: TONLE SAP WATER BALANCE. *Hydrological Processes*, *28*(4), 1722–1733. https://doi.org/10.1002/hyp.9718Lei, Y., Yang, K., Wang, B., Sheng, Y., Bird, B. W., Zhang, G., & Tian, L. (2014). Response of inland lake dynamics over the Tibetan Plateau to climate change. *Climatic Change*, *125*(2), 281–290. https://doi.org/10.1007/s10584-014-1175-3Li, D., Lu, X., Walling, D. E., Zhang, T., Steiner, J. F., Wasson, R. J., et al. (2022). High Mountain Asia hydropower systems threatened by climate-driven landscape instability. *Nature Geoscience*. https://doi.org/10.1038/s41561-022-00953-yLi, Y., Liao, J., Guo, H., Liu, Z., & Shen, G. (2014). Patterns and Potential Drivers of Dramatic Changes in Tibetan Lakes, 1972–2010. *PLoS ONE*, *9*(11), e111890. https://doi.org/10.1371/journal.pone.0111890Lutz, A. F., Immerzeel, W. W., Shrestha, A. B., & Bierkens, M. F. P. (2014). Consistent increase in High Asia's runoff due to increasing glacier melt and precipitation. *Nature Climate Change*, *4*(7), 587–592. https://doi.org/10.1038/nclimate2237McFEETERS,

S. K. (1996). The use of the Normalized Difference Water Index (NDWI) in the delineation of open water features. *International Journal of Remote Sensing*, *17*(7), 1425–1432. https://doi.org/10.1080/01431169608948714McNally, A., Arsenault, K., Kumar, S., Shukla, S., Peterson, P., Wang, S., et al. (2017). A land data assimilation system for sub-Saharan Africa food and water security applications. *Scientific Data*, *4*(1), 170012. https://doi.org/10.1038/sdata.2017.12Messager, M. L., Lehner, B., Grill, G., Nedeva, I., & Schmitt, O. (2016). Estimating the volume and age of water stored in global lakes using a geo-statistical approach. *Nature Communications*, *7*(1), 13603. https://doi.org/10.1038/ncomms13603Micklin, P. (2016). The future Aral Sea: hope and despair. *Environmental Earth Sciences*, *75*(9), 844. https://doi.org/10.1007/s12665-016-5614-5Miles, E., McCarthy, M., Dehecq, A., Kneib, M., Fugger, S., & Pellicciotti, F. (2021). Health and sustainability of glaciers in High Mountain Asia. *Nature Communications*, *12*(1), 2868. https://doi.org/10.1038/s41467-021-23073-4Miles, K. E., Hubbard, B., Irvine-Fynn, T. D. L., Miles, E. S., Quincey, D. J., & Rowan, A. V. (2020). Hydrology of debris-covered glaciers in High Mountain Asia. *Earth-Science Reviews*, *207*, 103212. https://doi.org/10.1016/j.earscirev.2020.103212Ni, J., Wu, T., Zhu, X., Hu, G., Zou, D., Wu, X., et al. (2021). Simulation of the Present and Future Projection of Permafrost on the Qinghai-Tibet Plateau with Statistical and Machine Learning Models. *Journal of Geophysical Research: Atmospheres*, *126*(2). https://doi.org/10.1029/2020JD033402Nie, Y., Sheng, Y., Liu, Q., Liu, L., Liu, S., Zhang, Y., & Song, C. (2017). A regional-scale assessment of Himalayan glacial lake changes using satellite observations from 1990 to 2015. *Remote Sensing of Environment*, *189*, 1–13. https://doi.org/10.1016/j.rse.2016.11.008Panyushkina, I. P., Meko, D. M., Macklin, M. G., Toonen, W. H. J., Mukham diev, N. S., Konovalov, V. G., et al. (2018). Runoff variations in Lake Balkhash Basin, Central Asia, 1779–2015, inferred from tree rings. *Climate Dynamics*, *51*(7–8), 3161–3177. https://doi.org/10.1007/s00382-018-4072-zPekel, J. F., Cottam, A., Gorelick, N., & Belward, A. S. (2016). High-resolution mapping of global surface water and its long-term changes. *Nature*, *540*(7633). https://doi.org/10.1038/nature20584Ruan, Y., Zhang, X., Xin, Q., Qiu, Y., & Sun, Y. (2020). Prediction and Analysis of Lake Ice Phenology Dynamics Under Future Climate Scenarios Across the Inner Tibetan Plateau. *Journal of Geophysical Research: Atmospheres*, *125*(23). https://doi.org/10.1029/2020JD033082Shean, D. E., Bhushan, S., Montesano, P., Rounce, D. R., Arendt, A., & Osmanoglu, B. (2020). A Systematic, Regional Assessment of High Mountain Asia Glacier Mass Balance. *Frontiers in Earth Science*, *7*, 363. https://doi.org/10.3389/feart.2019.00363Shi, W., Wang, M., & Guo, W. (n.d.). Long-term hydrological changes of the Aral Sea observed by satellites. *Journal of Geophysical Research*, 14.Shugar, D. H., Burr, A., Haritashya, U. K., Kargel, J. S., Watson, C. S., Kennedy, M. C., et al. (2020). Rapid worldwide growth of glacial lakes since 1990. *Nature Climate Change*, *10*(10), 939–945. https://doi.org/10.1038/s41558-020-0855-4Smith, L. C., Sheng, Y., MacDonald, G. M., & Hinzman, L. D. (2005). Disappearing Arctic Lakes.

Science, *308*(5727), 1429–1429. https://doi.org/10.1126/science.1108142Song, C., Huang, B., Ke, L., & Richards, K. S. (2014). Remote sensing of alpine lake water environment changes on the Tibetan Plateau and surroundings: A review. *ISPRS Journal of Photogrammetry and Remote Sensing*, *92*, 26–37. https://doi.org/10.1016/j.isprsjprs.2014.03.001Tandong Y., Fahu C., Peng C., Yaoming M., Baiqing X., Liping Z., et al. (n.d.). From Tibetan Plateau to Third Pole and Pan-Third Pole, 11.Tayfur, G., & Alami, M. M. (2022). Meteorological Drought Analysis for Helmand River Basin, Afghanistan. *Teknik Dergi*. https://doi.org/10.18400/tekderg.868595Veh, G., Korup, O., von Specht, S., Roessner, S., & Walz, A. (2019). Unchanged frequency of moraine-dammed glacial lake outburst floods in the Himalaya. *Nature Climate Change*, *9*(5), 379–383. https://doi.org/10.1038/s41558-019-0437-5Wan, W., Long, D., Hong, Y., Ma, Y., Yuan, Y., Xiao, P., et al. (2016). A lake data set for the Tibetan Plateau from the 1960s, 2005, and 2014. *Scientific Data*, *3*(1), 160039. https://doi.org/10.1038/sdata.2016.39Wang, X., Guo, X., Yang, C., Liu, Q., Wei, J., Zhang, Y., et al. (2020). Glacial lake inventory of high-mountain Asia in 1990 and 2018 derived from Landsat images. *Earth System Science Data*, *12*(3), 2169–2182. https://doi.org/10.5194/essd-12-2169-2020Wester, P., Mishra, A., Mukherji, A., & Shrestha, A. B. (Eds.). (2019). *The Hindu Kush Himalaya Assessment: Mountains, Climate Change, Sustainability and People*. Cham: Springer International Publishing. https://doi.org/10.1007/978-3-319-92288-1Woolway, R. I., Kraemer, B. M., Lenters, J. D., Merchant, C. J., O'Reilly, C. M., & Sharma, S. (2020). Global lake responses to climate change. *Nature Reviews Earth & Environment*, *1*(8), 388–403. https://doi.org/10.1038/s43017-020-0067-5Wu, G., Chen, J., Shi, X., Kim, J., Xia, J., & Zhang, L. (2022). Impacts of Global Climate Warming on Meteorological and Hydrological Droughts and Their Propagations. *Earth's Future*, *10*(3). https://doi.org/10.1029/2021EF002542Yan, Y., You, Q., Wu, F., Pepin, N., & Kang, S. (2020). Surface mean temperature from the observational stations and multiple reanalyses over the Tibetan Plateau. *Climate Dynamics*, *55*(9–10), 2405–2419. https://doi.org/10.1007/s00382-020-05386-0Yang, X., Wang, N., Chen, A., He, J., Hua, T., & Qie, Y. (2020). Changes in area and water volume of the Aral Sea in the arid Central Asia over the period of 1960–2018 and their causes. *CATENA*, *191*, 104566. https://doi.org/10.1016/j.catena.2020.104566Yao, T., Xue, Y., Chen, D., Chen, F., Thompson, L., Cui, P., et al. (2019). Recent Third Pole's Rapid Warming Accompanies Cryospheric Melt and Water Cycle Intensification and Interactions between Monsoon and Environment: Multidisciplinary Approach with Observations, Modeling, and Analysis. *Bulletin of the American Meteorological Society*, *100*(3), 423–444. https://doi.org/10.1175/BAMS-D-17-0057.1Yao, T., Bolch, T., Chen, D., Gao, J., Immerzeel, W., Piao, S., et al. (2022). The imbalance of the Asian water tower. *Nature Reviews Earth & Environment*. https://doi.org/10.1038/s43017-022-00299-4You, Q., Cai, Z., Pepin, N., Chen, D., Ahrens, B., Jiang, Z., et al. (2021). Warming amplification over the Arctic Pole and Third Pole: Trends, mechanisms and consequences. *Earth-Science Reviews*, *217*, 103625. https://doi.org/10.1016/j.earscirev.2021.103625Zhang,

G., Yao, T., Xie, H., Zhang, K., & Zhu, F. (2014). Lakes' state and abundance across the Tibetan Plateau. *Chinese Science Bulletin*, *59*(24), 3010–3021. https://doi.org/10.1007/s11434-014-0258-xZhang, G., Yao, T., Piao, S., Bolch, T., Xie, H., Chen, D., et al. (2017). Extensive and drastically different alpine lake changes on Asia's high plateaus during the past four decades: Lake Changes in the MP and TP. *Geophysical Research Letters*, *44*(1), 252–260. https://doi.org/10.1002/2016GL072033Zhang, G., Yao, T., Shum, C. K., Yi, S., Yang, K., Xie, H., et al. (2017). Lake volume and groundwater storage variations in Tibetan Plateau's endorheic basin. *Geophysical Research Letters*, *44*(11), 5550–5560. https://doi.org/10.1002/2017GL073773Zhang, G., Luo, W., Chen, W., & Zheng, G. (2019). A robust but variable lake expansion on the Tibetan Plateau. *Science Bulletin*, *64*(18), 1306–1309. https://doi.org/10.1016/j.scib.2019.07.018Zhang, G., Yao, T., Xie, H., Yang, K., Zhu, L., Shum, C. K., et al. (2020). Response of Tibetan Plateau lakes to climate change: Trends, patterns, and mechanisms. *Earth-Science Reviews*, *208*, 103269. https://doi.org/10.1016/j.earscirev.2020.103269Zhang, Y., Zhang, G., & Zhu, T. (2020). Seasonal cycles of lakes on the Tibetan Plateau detected by Sentinel-1 SAR data. *Science of The Total Environment*, *703*, 135563. https://doi.org/10.1016/j.scitotenv.2019.135563Zhao, G., Li, Y., Zhou, L., & Gao, H. (2022). Evaporative water loss of 1.42 million global lakes. *Nature Communications*, *13*(1), 3686. https://doi.org/10.1038/s41467-022-31125-6Zheng, G., Allen, S. K., Bao, A., Ballesteros-Cánovas, J. A., Huss, M., Zhang, G., et al. (2021). Increasing risk of glacial lake outburst floods from future Third Pole deglaciation. *Nature Climate Change*, *11*(5), 411–417. https://doi.org/10.1038/s41558-021-01028-3